24th COBEM - 2017

24th ABCM International Congress of Mechanical Engineering
December 3-8, 2017, Curitiba, PR, Brazil

COBEM-2017-0601
DYNAMIC RESPONSE ANALYSIS OF STEEL CATENARY RISERS UNDER THE INFLUENCE OF AN INTERNAL SLUG FLOW

Joseph Arthur Meléndez Vásquez
National Institute for Space Research - INPE
j.melendez.v@hotmail.com

Juan Pablo Julca Avila
Federal University of ABC - UFABC
j.avila@ufabc.edu.br

Abstract. *Slug flow through marine risers is a frequent phenomenon that occurs during the production of oil and gas. The dynamic nature of the slug flow induces time-dependent forces on the steel catenary riser, thus affecting its structural dynamic response. The purpose of this work is a two-dimensional analysis of the structural dynamic response of steel catenary risers under the influence of an internal slug flow. To accomplish this goal, a computational tool is developed. The spatial discretization of the riser is performed using beam finite elements and the corotational approach is used for the two-dimensional formulation of the beam element. The beam elements have a linear elastic behaviour and they are submitted to large displacements, although with small deformations. The incremental-iterative Newton-Raphson scheme for follower loads is used to solve the equilibrium equations in static and dynamic analysis. Time domain numerical integration is performed using the constant average acceleration method. The slug flow is viewed as a single-phase fluid with variable density, which is modelled by a periodic function. It has been found that variations in slug flow frequencies has a higher impact on the response amplitude of the top tension at higher values of liquid mass flow.*

Keywords: *structural dynamic response, large displacements, corotational formulation, slug flow.*

1. INTRODUCTION

In oil and gas exploration and production operations in deep and ultra-deep water, steel catenary risers (SCRs) are widely used to connect a subsea pipeline to a deep water floating or fixed oil production platform. Because their high resistance to external and internal pressures when exposed at great depths, SCRs have become the primary candidates to be used with floating production platforms in future ultra-deep water operations of the oil and gas industry.

The internal fluid moving inside the riser is a mixture of oil, gas, and water, and it is exposed to different conditions of pressure and temperature that enable the formation of emulsions, hydrates, and waxes. These characteristics make the modelling of the internal fluid a highly complex task. When a two-phase fluid, composed of gas and liquid, flows upward in a riser, the two phases may distribute in a variety of flow patterns. In this work, the slug flow is considered as the pattern of the internal fluid.

In order to understand the effect produced by the slug flow on the dynamics of risers, analytical and experimental works were performed in the last years. Patel and Seyed (1989) proposed a simplified one-dimensional model based on the sinusoidal behaviour of the internal fluid density along the riser. Valdivia (2008) carried out an experimental study, in which a silicone pipe was used with an internal fluid composed of water and air. Ortega (2015) used a computational tool to predict the development of the slug flow using a lagrangian tracking model (LASSI).

2. TWO-DIMENSIONAL FORMULATION FOR BEAMS

For the two-dimensional formulation of beams, the corotational approach, formulated by Yaw (2009) has been used. The beam element is considered as a structure that performs two types of movement, translation and rotation; after that, it suffers deformations caused by its internal forces.

From Fig. 1, the beam element in its initial configuration is defined by the global nodal coordinates (x_1, y_1) for node 1, and (x_2, y_2) for node 2. In its current configuration, the node number 1 of the beam element is defined by (x_1+u_1, y_1+v_1) and θ_1, and the node number 2 is defined by $(x_2 + u_2, y_2 + v_2)$ and θ_2, where u_1 and v_1 are the horizontal and vertical displacement of node 1, respectively, u_2 and v_2 are the horizontal and vertical displacement of node 2, and θ_1 and θ_2 are the rotation angles of the nodes number 1 and 2, respectively, which are measured starting from its initial position. Two

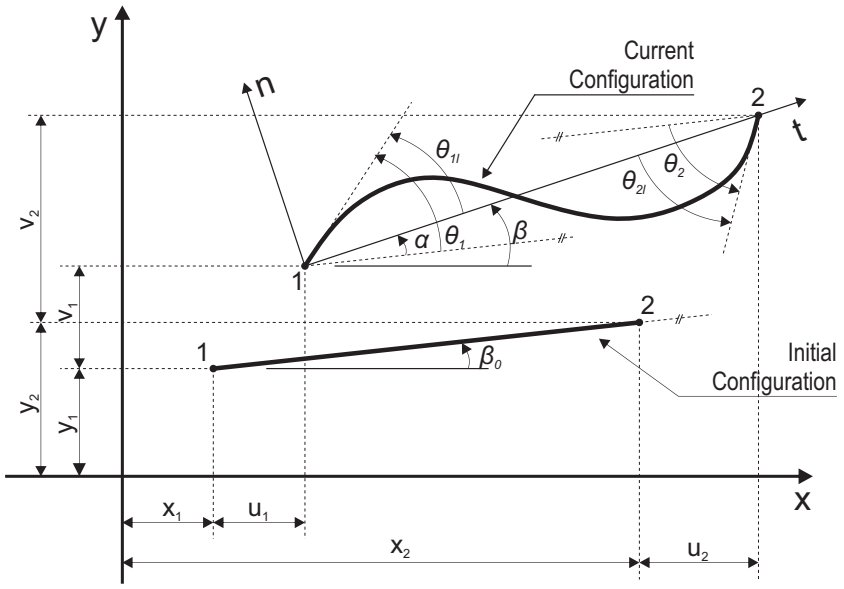

Figure 1. Initial and current configuration of a beam element.

coordinates systems are used in the corotational approach, the global coordinate system $(\mathbf{x}, \mathbf{y})$ and the local corotating coordinate system $(\mathbf{t}, \mathbf{n})$, where the direction of $\mathbf{t}$ is given by the straight line between the nodal points 1 and 2 in the current configuration.

From Fig. 1, the global displacement vector $\mathbf{u}$ and the local displacement vector $\mathbf{u_l}$ are defined as the following:

$$\mathbf{u} = \begin{Bmatrix} u_1 & v_1 & \theta_1 & u_2 & v_2 & \theta_2 \end{Bmatrix}^T \tag{1}$$

$$\mathbf{u_l} = \begin{Bmatrix} \bar{u} & \theta_{1l} & \theta_{2l} \end{Bmatrix}^T \tag{2}$$

where $\bar{u}$ is the local axial displacement of the beam element, θ_{1l} and θ_{2l} are the local rotations of nodes 1 and 2, respectively. The components of $\mathbf{u_l}$ are calculated according to:

$$\bar{u} = L - L_o \tag{3}$$

$$\theta_{ll} = \theta_1 - \beta + \beta_o \tag{4}$$

$$\theta_{2l} = \theta_2 - \beta + \beta_o \tag{5}$$

From Eqs. (3), (4), and (5), L_o and L are the measures of the distance between the nodes 1 and 2 in the initial and the current configuration of the beam element, respectively, and β_o and β are the measures of the inclination of the local coordinates system in its initial and current configuration, respectively, with regards to the global coordinates system. The variables L_o, L, β_o and β can be calculated as a function of the global nodal coordinates (x_1, x_2, y_1 and y_2) and the horizontal and vertical displacements (u_1, u_2, v_1 and v_2).

Applying the variational operator on the Eqs. (3), (4), and (5), the following relationship between the local and global variables is obtained:

$$\delta\mathbf{u_l} = \mathbf{B}\delta\mathbf{u} \tag{6}$$

where the matrix **B** is defined by

$$\mathbf{B} = \begin{bmatrix} -cos\beta & -sin\beta & 0 & cos\beta & sin\beta & 0 \\ -sin\beta/L & cos\beta/L & 1 & sin\beta/L & -cos\beta/L & 0 \\ -sin\beta/L & cos\beta/L & 0 & sin\beta/L & -cos\beta/L & 1 \end{bmatrix} \tag{7}$$

2.1 Calculus of the tangent stiffness matrix of a beam element

The amount of virtual work performed by the acting forces on the beam element in the global and local coordinates systems is equivalent, and thus, the following relationship is valid:

$$\delta \mathbf{u}^{\mathbf{T}} \mathbf{q} = \delta \mathbf{u_l}^{\mathbf{T}} \mathbf{q_l} \tag{8}$$

Substituting Eq. (6) in the right side of Eq. (8), the following equation, that relates the local force vector and the global force vector, is obtained:

$$\mathbf{q} = \mathbf{B}^{\mathbf{T}} \mathbf{q_l} \tag{9}$$

where $\mathbf{q}$ and $\mathbf{q_l}$ are the vectors of global and local internal forces acting on the beam element, respectively. The vector of local internal forces contains the axial force N, which is considered constant along the beam element, and the local end moments $\bar{M}_1$ and $\bar{M}_2$, acting on the nodal points 1 and 2, respectively. The vector of local forces is given by:

$$\mathbf{q_l} = \begin{Bmatrix} N & \bar{M}_1 & \bar{M}_2 \end{Bmatrix}^T \tag{10}$$

where its components N, $\bar{M}_1$ and $\bar{M}_2$ are computed as:

$$N = \frac{EA\bar{u}}{L_o} \tag{11}$$

$$\begin{Bmatrix} \bar{M}_1 \\ \bar{M}_2 \end{Bmatrix} = \frac{2EI}{L_o} \begin{bmatrix} 2 & 1 \\ 1 & 2 \end{bmatrix} \begin{Bmatrix} \theta_{1l} \\ \theta_{2l} \end{Bmatrix} \tag{12}$$

where E is the modulus of elasticity and I is the second moment of area of the cross section of a beam element. By applying the variational operator to Eq. (9) and some mathematical manipulations, the tangent stiffness matrix $\mathbf{k_t}$ for a beam element is obtained:

$$\mathbf{k_t} = \mathbf{B}^{\mathbf{T}} \mathbf{C_l} \mathbf{B} + \left(\frac{N}{L} \right) \mathbf{z}\mathbf{z}^{\mathbf{T}} + \left(\frac{\bar{M}_1 + \bar{M}_2}{L^2} \right) \left(\mathbf{r}\mathbf{z}^{\mathbf{T}} + \mathbf{z}\mathbf{r}^{\mathbf{T}} \right) \tag{13}$$

where $\mathbf{C_l}$, $\mathbf{z}$, and $\mathbf{r}$ are defined by:

$$\mathbf{C_l} = \frac{EA}{L_0} \begin{bmatrix} 1 & 0 & 0 \\ 0 & 4r^2 & 2r^2 \\ 0 & 2r^2 & 4r^2 \end{bmatrix} \tag{14}$$

$$\mathbf{z} = \begin{bmatrix} \sin\beta & -\cos\beta & 0 & -\sin\beta & \cos\beta & 0 \end{bmatrix}^T \tag{15}$$

$$\mathbf{r} = \begin{bmatrix} -\cos\beta & -\sin\beta & 0 & \cos\beta & \sin\beta & 0 \end{bmatrix}^T \tag{16}$$

where A is the cross-sectional area of the beam element, and r is the radius of gyration, which is defined as $r = \sqrt{I/A}$.

2.2 Local displacements of a beam element

The local displacements considered for a point P of the beam element are the local transverse displacement w and the local rotation θ_l. The local transverse displacement w is approximated using the conventional cubic polynomial, being the values of w zero at the two ends. Thus, w and θ_l would be expressed as

$$w = \left(s - \frac{2s^2}{L} + \frac{s^3}{L^2} \right) \theta_{1l} + \left(-\frac{s^2}{L} + \frac{s^3}{L^2} \right) \theta_{2l} \tag{17}$$

$$\theta_l = \frac{dw}{ds} = \left(1 - \frac{4s}{L} + \frac{3s^2}{L^2} \right) \theta_{1l} + \left(-\frac{2s}{L} + \frac{3s^2}{L^2} \right) \theta_{2l} \tag{18}$$

From Eq. (17) and Eq. (18), s is the local coordinate in the tangential direction, and L is the length of the beam element in the current configuration (see Fig. 1).

3. ACTING LOADS ON A STEEL CATENARY RISER

The acting loads on an element of SCR are shown in Fig. 2.

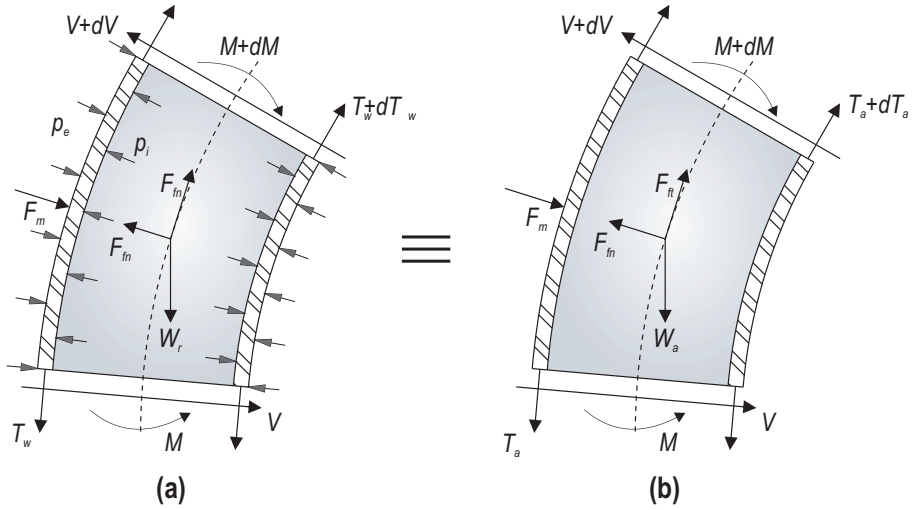

Figure 2. (a) Acting loads over an element of SCR. (b) Equivalent forces system acting over an element of SCR.

- p_e is the external pressure due to the seawater, and p_i is the internal pressure due to the internal fluid.
- T_w is the true wall tension, V is the shear force, and M is the bending moment.
- F_{fn} and F_{ft} are the acting forces due to the internal fluid in the normal and tangential direction to the riser element axis, respectively.
- F_m is the force due to the current. The force caused by the current is calculated using the Morison equation, for which the normal component approach is used. The normal component approach considers that the normal forces to the SCR element are the predominant ones, whereas the tangential forces are not taken into account.
- W_r is the own weight of the riser.

Figure 2(b) shows an equivalent forces system, where T_a is the apparent tension acting on the riser, and W_a is the apparent weight of the riser. The procedure to obtain the equivalent forces system has been performed by Chucheepsakul *et al.* (2003).

3.1 Apparent tension

In a production riser, fluids act internally and externally, generating hydrostatic, static, and dynamic pressures. The concept of apparent tension is proposed by Chucheepsakul *et al.* (2003) with the purpose of represent the combined effect of the external and internal pressures and the true wall tension acting on an element of riser. The apparent tension, T_a, and the true wall tension, T_w, are related by means of the following equation:

$$\mathbf{T_a} = T_a\ \hat{\mathbf{t}} = \left[T_w + 2\nu\left(p_e A_e - p_i A_i\right)\right]\hat{\mathbf{t}} \tag{19}$$

where ν is the Poisson's coefficient, while A_e and A_i are the external and internal area of the transversal section of the riser, respectively. If the internal fluid is flowing with a velocity v, the following relationship is obtained:

$$\mathbf{T_a} = T_a\ \hat{\mathbf{t}} = \left[T_w + 2\nu\left(p_e A_e - p_i A_i - \rho_f v^2 A_i\right)\right]\hat{\mathbf{t}} \tag{20}$$

where ρ_f is the density of the internal fluid.

3.2 Apparent weight

The concept of apparent weight is used to represent the combined effect of the weight of the riser and the buoyancy forces owing to the external and internal fluids acting on the riser (Sparks, 1984). Considering a differential element of

length ds, the apparent weight of the riser element $(w_a ds)$ can be calculated by adding the Archimedian upthrust owing to the seawater $(\rho_w A_e g ds)$ and the weight of the contained fluid $(\rho_f A_e g ds)$ to the true weight of the pipe $(w_r ds)$. Then, the following relationship is obtained:

$$w_a = w_r + \rho_f A_i g - \rho_w A_e g \tag{21}$$

where w_a and w_r are the apparent weight and the true weight of the riser per unit of length, respectively, ρ_f is the density of the internal fluid, and ρ_w is the density of the seawater.

3.3 Loads due to the internal fluid

Consider a fluid finite system moving with a local velocity V and acceleration $\mathbf{a}$. The force applied by the internal fluid on the riser element can be calculated as

$$d\mathbf{F_f} = -\mathbf{a}.dm \tag{22}$$

where $\mathbf{F_f}$ is the force vector owing to the dynamics of the internal fluid and dm is a differential element of the fluid mass. From Eq. (22) and using $dm = \rho_f A_i ds$, the force owing to the internal fluid per unit of length of riser, $\mathbf{f_f}$, can be calculated as

$$\mathbf{f_f} = -\rho_f A_i \mathbf{a} \tag{23}$$

The acceleration of a fluid particle moving inside the riser is calculated using the expression given by Shames (2003):

$$\mathbf{a} = \mathbf{a_L} + \ddot{\mathbf{R}} + 2\boldsymbol{\omega} \times \mathbf{V} + \dot{\boldsymbol{\omega}} \times \mathbf{r} + \boldsymbol{\omega} \times (\boldsymbol{\omega} \times \mathbf{r}) \tag{24}$$

where $\mathbf{a}$ is the acceleration in the global system of coordinates $(\mathbf{x}, \mathbf{y}, \mathbf{z})$ and $\mathbf{a_L}$ is the acceleration in the local coordinate system $(\mathbf{t}, \mathbf{n}, \mathbf{b})$ (see Fig. **??**). On the right side of the Eq. (24), the third term represents the Coriolis acceleration, the fourth term represents the acceleration caused by the angular acceleration of the local system $(\mathbf{t}, \mathbf{n}, \mathbf{b})$, and the fifth term represents the centripetal acceleration.

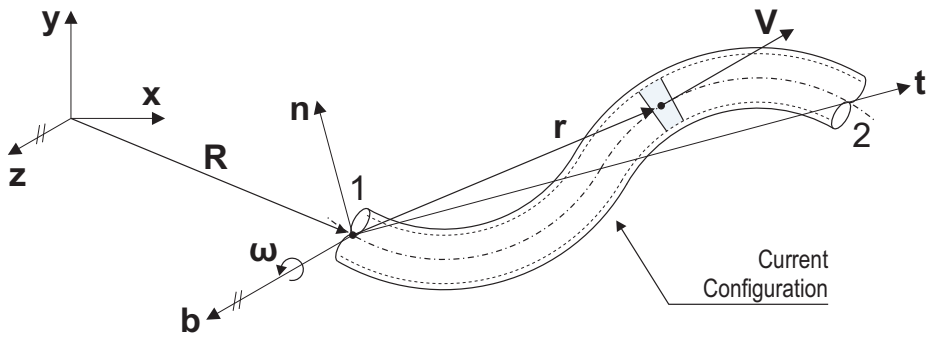

Figure 3. Fluid particle moving through an element of riser.

The velocity of the slug flow, V, will be defined once the mathematical model is known. The model to represent the slug flow will be treated below.

3.3.1 Mathematical model of slug flow

The slug flow is characterized by large bubbles of gas, also called Taylor bubbles, which have a diameter almost equal to the riser diameter, separated by slugs of continuous liquid, which contain small gas bubbles, as showed in Fig. 3.

From Fig. 3, D_e and D_i are the external and internal diameter of the SCR, respectively, l_l and l_g are the length of the liquid slug and the Taylor bubble, respectively, and l_s is the slug wavelength.

To represent the changes in density of the slug flow, owing to the mixture of gas and liquid phases, the slug flow was modelled as a single-phase fluid having a variable density, which varies periodically in relation to the arc length and to the moment in time. In this work, the mathematical model used is the one proposed by Patel and Seyed (1989), which is expressed by the following equation:

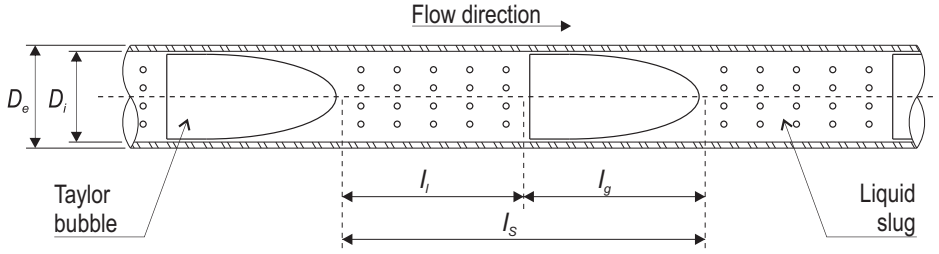

Figure 4. Slug flow geometry.

$$\rho_f = \rho_o + \rho_s \sin(\kappa s + \psi)\, e^{i\omega t} \tag{25}$$

where ρ_o is the average density between the liquid phase density (ρ_l) and the gas phase density (ρ_g), ρ_s is the amplitude of density variations, $\kappa(= 2\pi/ls)$ is the slug wave number, s is the arc length of the riser at this point, ω is the slug circular frequency and ψ is the angle phase.

Once the geometry of the slug flow is known, we proceed to calculate the velocity of a slug flow particle. To do that, we start by calculating the total mass flow rate of the slug flow, which is calculated for a mixture of water and gas as

$$\dot{m} = Q_l.\rho_l + Q_g.\rho_g \tag{26}$$

where Q_l and Q_g are the volumetric flow rate of liquid and gas, respectively. From the work of Santos (2006) and Taitel *et al.* (1980), the flow rates of liquid and gas can be expressed as a function of the liquid superficial velocities, V_{sl}, and the gas superficial velocity, V_{sg}, as follows:

$$Q_l = V_{sl}A_i \quad , \quad Q_g = V_{sg}A_i \tag{27}$$

The local velocity of a fluid particle of slug flow can be calculated using the continuity equation (conservation of mass); then, substituting variables, the following equation is obtained:

$$V = \frac{V_{sl}\rho_l + V_{sg}\rho_g}{\rho_f} \tag{28}$$

The concept of mixing velocity, V_m, is introduced by Taitel *et al.* (1980), and can expressed as

$$V_m = V_{sl} + V_{sg} \tag{29}$$

The mixing velocity can be used to link the slug wavelength and the slug circular frequency by means of the following equation:

$$l_s = V_m/\omega \tag{30}$$

3.4 Loads due to the current

The hydrodynamic loads caused by the current acting on a slanting cylinder can be calculated by using the Morison equation. In this work, as mentioned before, the normal component approach will be used, which considers that only velocities and accelerations normal to the SCR element generate forces, without taking into account the effect of the tangential forces.

From Fig. 4, V_c is the current velocity, V_t and V_n are the current velocity in the tangent and normal direction, respectively, $\dot{u}_n$ and $\ddot{u}_n$ are the components of velocity and acceleration of the riser in the normal direction to the cylinder axis, respectively, and f_m is the Morison's force per unit of length.

The force caused by the current per unit of length is expressed by (see Patel (2013))

$$f_m = \frac{1}{2}C_D\rho_w D_e|v_n - \dot{u}_n|\,(v_n - \dot{u}_n) + C_M\rho_w\dot{v}_n\frac{\pi D_e^2}{4} - C_A\rho_w\ddot{u}_n\frac{\pi D_e^2}{4} \tag{31}$$

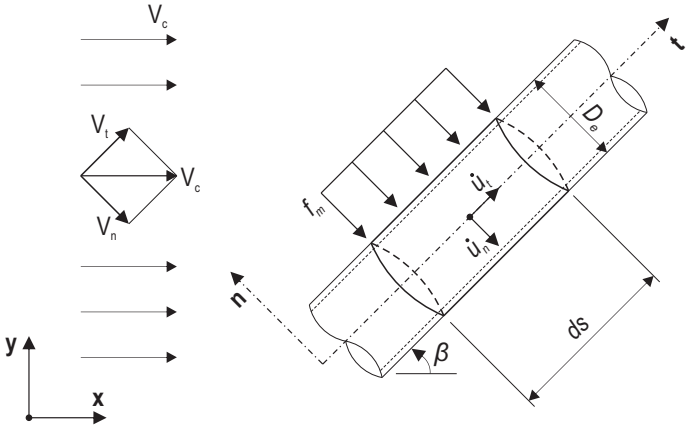

Figure 5. Morison's force over a slanting cylinder.

where C_D, C_M, and C_A are the drag, inertia, and added mass coefficients, respectively, and ρ_w is the density of seawater. $\dot{v}_n$ is the component of the acceleration of the seawater in the normal direction to the cylinder axis.

In Eq. (31), the first term on the right side of the equation represents the drag forces, the second term represents the inertia forces, and the third term represents the forces caused by the added masses.

4. NUMERICAL METHODS

The dynamic response of a SCR, the objective of this paper, is calculated from its static equilibrium configuration. In this section, the equilibrium equations for the static and dynamic analysis are presented.

4.1 Static analysis

The static equilibrium configuration of a SCR is obtained from the solution of the following equilibrium equation:

$$\mathbf{R}_{\mathrm{t}} - \mathbf{Q}_{\mathrm{t}} = \mathbf{0} \tag{32}$$

where the vector $\mathbf{R}_{\mathrm{t}}$ lists the externally applied nodal point forces in the configuration at time t and the vector $\mathbf{Q}_{\mathrm{t}}$ lists the internal nodal forces. The external force vector $\mathbf{R}_{\mathrm{t}}$ is composed of the apparent weight, loads owing to the internal fluid, and loads owing to the current, which are expressed by Eq. (21), Eq. (23), and Eq. (31), respectively, with the following considerations:

$$\dot{\mathbf{U}} = \ddot{\mathbf{U}} = \mathbf{0} \tag{33}$$

where $\dot{\mathbf{U}}$ and $\ddot{\mathbf{U}}$ are the nodal velocity vector and the nodal acceleration vector, respectively. The Newton-Raphson method is utilized for the solution of Eq. (32) (see Chopra (2012)).

4.2 Dynamic analysis

The dynamic response of a SCR, at a given time t, is obtained from the solution of the following dynamic equilibrium equation:

$$\mathbf{M}_{\mathrm{t}}\ddot{\mathbf{U}}_{\mathrm{t}} + \mathbf{C}_{\mathrm{t}}\dot{\mathbf{U}}_{\mathrm{t}} + \mathbf{Q}_{\mathrm{t}}\left(\mathbf{U}_{\mathrm{t}}\right) = \mathbf{P}_{\mathrm{t}}\left(\dot{\mathbf{U}}_{\mathrm{t}}, \mathbf{U}_{\mathrm{t}}, \mathrm{t}\right) \tag{34}$$

associated with the initial conditions at time $t = 0$:

$$\mathbf{U}_{\mathrm{t}=0} = \mathbf{U}_0 = \mathbf{0} \quad \text{and} \quad \dot{\mathbf{U}}_{\mathrm{t}=0} = \dot{\mathbf{U}}_0 = \mathbf{0} \tag{35}$$

where $\mathbf{M}$ is the global mass matrix, that is the sum of the global matrix of mass-structure $\mathbf{M}_{\mathrm{scr}}$ and the global matrix of added mass $\mathbf{M}_{\mathrm{add}}$. $\mathbf{C}$ is the structural damping matrix and $\mathbf{Q}$ is the global vector of internal nodal forces owing to node displacements. The matrix $\mathbf{C}$ is estimated using the Rayleigh damping. $\mathbf{P}$ is the global external force vector applied at the nodes of structure. $\mathbf{U}$, $\dot{\mathbf{U}}$, and $\ddot{\mathbf{U}}$ are the global vectors of nodal displacement, velocity, and acceleration, respectively.

The constant average acceleration method is used to determine the dynamic response of SCR (see Chopra (2012)).

5. NUMERICAL RESULTS

In this section will be shown the numerical results obtained for the top tension applied in a SCR of real dimensions. The top tension was calculated for several values of slug flow frequencies, as well as for several values of the gaseous phase density. The geometric characteristics and mechanical properties of the SCR used in the simulations are listed in Tab. 1.

Table 1. Geometric characteristics and mechanical properties of the simulated riser.

Properties of simulated riser	Values
Riser length (m)	450
External diameter (m)	0.40
Internal diameter (m)	0.36
Effective weight (kN/m)	0.59
Elasticity modulus ($\mathrm{GN/m^2}$)	206
Bending stiffness ($\mathrm{kN.m^2}$)	8900
Poisson's coefficient	0.5
Damping ratio (%)	1

In this work, we consider that the riser is immersed in still water, in other words, with a current velocity equal to zero. For this reason, in the calculation of the dynamic response, only the drag force and the forces caused by the added masses from Eq. (31) are considered.

In the model simulations, the internal fluid will be represented as a mixture of water and gas. The density of water is $998\ \mathrm{kg/m^3}$. In the case of the gaseous phase, air is used and we consider that the gas behaves as an ideal gas, which is pressurized between 2000 and 5000 psi and operates at a temperature of 298 K. The density of the gaseous phase will be considered to have a value of $200\ \mathrm{kg/m^3}$. An average production capacity of the riser of 180000 BPD (barrels per day) is taken into consideration to estimate the values of the liquid and gas mass flows.

The depth of the sea is 300 meters with a density of $1025\ \mathrm{kg/m^3}$. For the present calculations, the drag and the added masses coefficients of the sea were considered as 0.7 and 1.0, respectively. To determine the static configuration, a horizontal force of 80 kN was applied to the top.

In the present analysis several cases are considered. It is important to point out that in every simulated case, the slug flow frequency was considered constant along the riser and at every moment in time. In the numerical simulations a simulation time of 500 s was considered.

5.1 Analysis of the apparent top tension for different values of slug flow frequencies

Several simulations were carried out in each of which were modified the value of the slug flow frequency. For the analysis, an interval of 25 s before the end of simulation was showed.

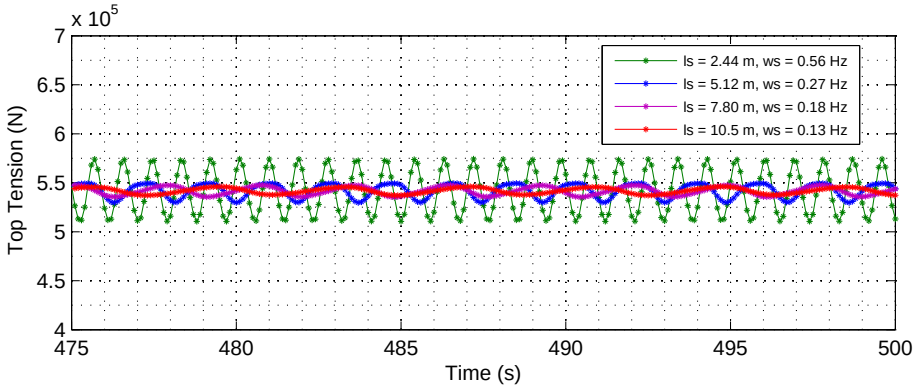

Figure 6. Top tension: $m_l = 100kg/s$, $m_g = 8kg/s$.

Figures 5, 6, 7 and 8, shows that the variations of the slug flow frequency causes variations in the top tension amplitude. Additionally, the top tension amplitudes are higher when the system operates with high values of liquid mass flow.

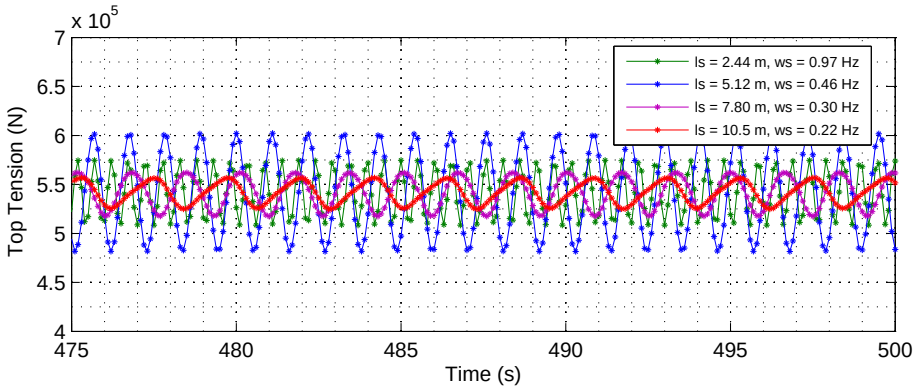

Figure 7. Top tension: $m_l = 200kg/s$, $m_g = 8kg/s$.

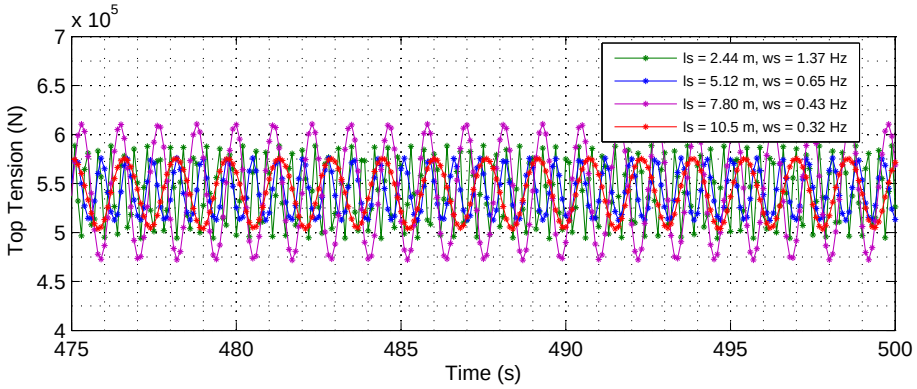

Figure 8. Top tension: $m_l = 300kg/s$, $m_g = 8kg/s$.

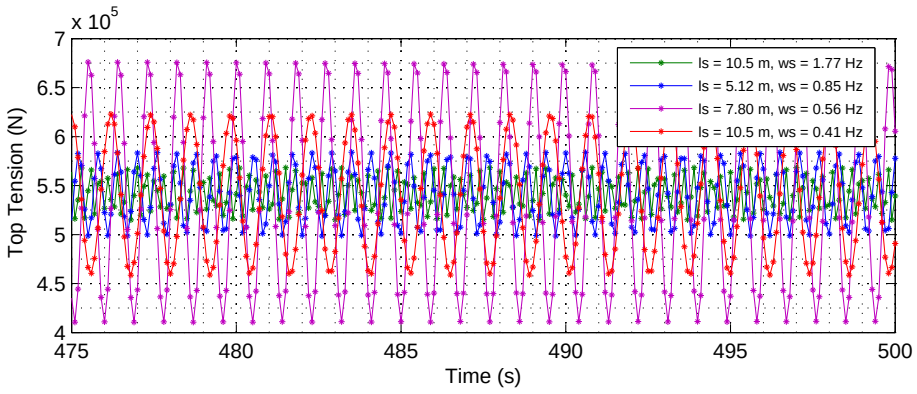

Figure 9. Top tension: $m_l = 400kg/s$, $m_g = 8kg/s$.

5.2 Analysis of the top tension for different values of gas density

Simulations were carried out to understand the effect of the gaseous phase density on the dynamic response of the top tension.

Figures 9, 10, 11 and 12, shows that by increasing the gaseous phase density of the internal fluid, the average top tension is increased, which is only natural because the weight of the internal fluid was increased. Other results that can be observed, as seen in the previous subsection, is that the response of the top tension is higher when the system operates with high values of liquid mass flow.

6. CONCLUSIONS

On the basis of the results, we can concluded the following:

1. In riser systems, when working with high values of liquid mass flow, large amplitudes in the dynamic response of the top tension may occur.

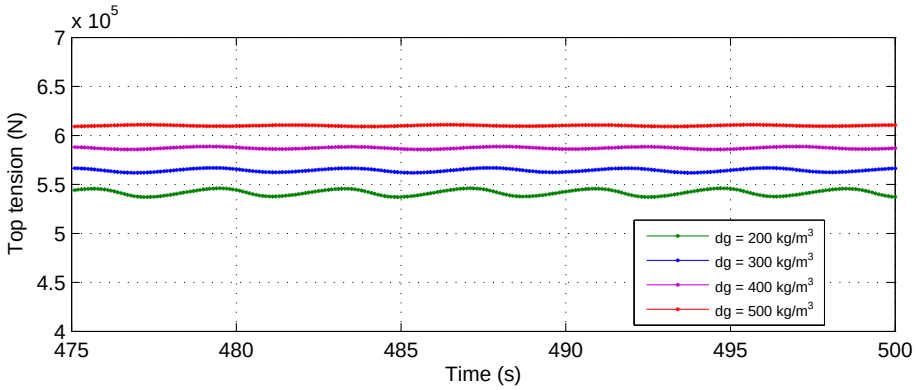

Figure 10. Top tension: $m_l = 100kg/s$, $m_g = 8kg/s$.

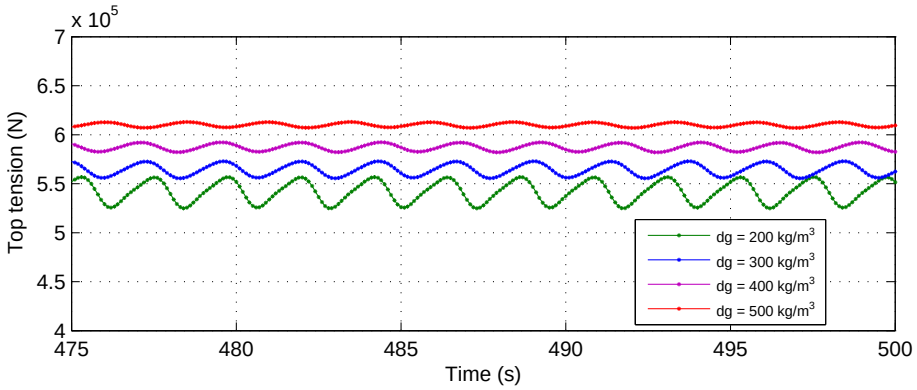

Figure 11. Top tension: $m_l = 200kg/s$, $m_g = 8kg/s$.

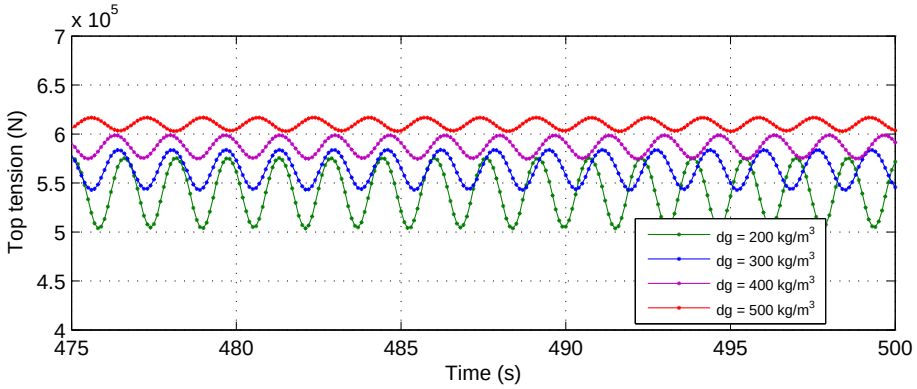

Figure 12. Top tension: $m_l = 300kg/s$, $m_g = 8kg/s$.

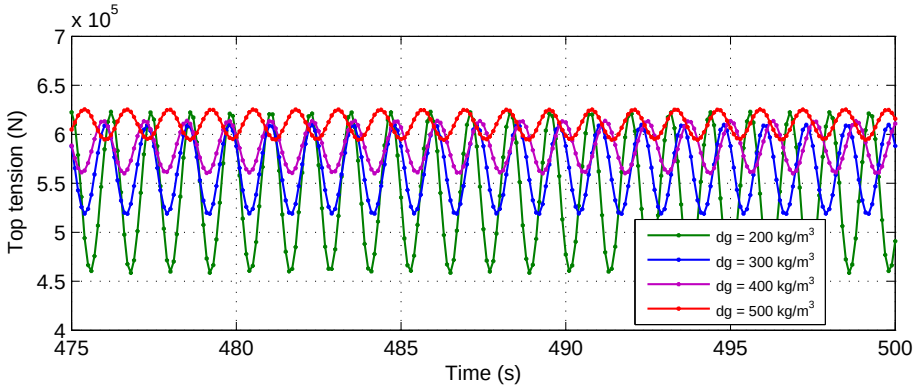

Figure 13. Top tension: $m_l = 400kg/s$, $m_g = 8kg/s$.

2. In a real riser occur constant variations in the amplitude of the top tension, because the slug flow frequency varies constantly along the riser.

7. ACKNOWLEDGEMENTS

The authors gratefully acknowledge the financial support by the Coordination for the Improvement of Higher Education Personnel (CAPES) and the National Institute for Space Research (INPE). The authors are also grateful to the Federal University of ABC (UFABC) for the use of their facilities for carrying out this work.

8. REFERENCES

Chopra, A.K., 2012. *Dynamics of structures: theory and applications to earthquake engineering*. Prentice-Hall, 4th edition.

Chucheepsakul, S., Monprapussorn, T. and Huang, T., 2003. "Large strain formulations of extensible flexible marine pipes transporting fluid". *Journal of Fluids and Structures*, Vol. 17, No. 2, pp. 185–224.

Ortega, A., 2015. *Dynamic response of flexible risers due to unsteady slug flow*. Ph.D. thesis, Norwegian University of Science and Technology, Norway.

Patel, M. and Seyed, F., 1989. "Internal flow-induced behaviour of flexible risers". *Engineering Structures*, Vol. 11, No. 4, pp. 266–280.

Patel, M.H., 2013. *Dynamics of offshore structures*. Butterworth-Heinemann.

Santos, E., 2006. *Estudo do escoamento bifásico em risers em movimento na produção maritima de petroleo em aguas profundas*. Master's thesis, State University of Campinas, São Paulo.

Shames, I., 2003. *Mechanics of fluids*. McGraw-Hill New York, 4th edition.

Sparks, C., 1984. "The influence of tension, pressure and weight on pipe and riser deformations and stresses". *Transactions of the ASME. Journal of Energy Resources Technology*, Vol. 106, No. 1, pp. 46–54.

Taitel, Y., Bornea, D. and Dukler, A., 1980. "Modelling flow pattern transitions for steady upward gas-liquid flow in vertical tubes". *AIChE Journal*, Vol. 26, No. 3, pp. 345–354.

Valdivia, P., 2008. *Estudo experimental e numerico da dinamica de movimento de riser em catenaria com escoamento interno*. Master's thesis, State University of Campinas, São Paulo.

Yaw, L., 2009. "2d corotational beam formulation".

9. RESPONSIBILITY NOTICE

The following text, properly adapted to the number of authors, must be included in the last section of the paper:
The author(s) is (are) the only responsible for the printed material included in this paper.